Journal of Catalysis **195,** 217–226 (2000)
doi:10.1006/jcat.2000.3007, available online at http://www.idealibrary.com on IDEAL®

A Novel Application of Trapping Catalysts for the Selective Low-Temperature Oxidation of NH_3 to N_2 in Simulated Biogas

R. Burch and B. W. L. Southward[1]

School of Chemistry, The Queen's University of Belfast, Belfast BT9 5AG, Northern Ireland, United Kingdom

Received May 22, 2000; revised July 21, 2000; accepted July 21, 2000

The low-temperature selective oxidation of NH_3 to N_2 in simulated biogas containing a large excess of CO and H_2 has been examined using a novel NH_3 and a standard NO_x trapping catalyst. The N_2 selectivity during NH_3 oxidation at 200°C for a 1%Pt–20%BaO–Al_2O_3 NO_x trapping material, with typical lean/rich switches, was initially good (>90%) but decreased markedly over a small number of cycles. In contrast, the N_2 yield obtained using a novel NH_3 trapping material (1%Pt–20%CuO–Al_2O_3) with rich/lean fuel switching exceeded 95% and was stable over many switching cycles, while an unmodified 1%Pt–Al_2O_3 catalyst displayed poor N_2 selectivity under all conditions. The data obtained from probe reactions between the various potential adsorbates and gaseous species of the reaction indicate that the N_2 yields obtained from the 1% Pt–20% CuO–Al_2O_3 catalyst are formed via an Internal Selective Catalytic Reduction (*i*SCR) between NH_x species adsorbed on the trapping component and NO formed from NH_3 total oxidation on the Pt during the lean cycle of operation. For the 1%Pt–20%BaO–Al_2O_3 catalyst, NO_x, formed during lean operation, is reduced to N_2 in the rich cycle by a combination of reactions with NH_3, CO, and H_2. The use of a hybrid catalyst, based upon a combination of *i*SCR and NO_x trapping processes, gave a peak N_2 yield of >95% and an integrated N_2 production over the entire rich/lean cycle of 75%. These results reflect the potentially dramatic improvements possible by rational design of catalyst systems based upon a fundamental knowledge of the processes involved.

Key Words: **biomass; heterogeneous catalyst; selective NH_3 oxidation; trapping.**

1. INTRODUCTION

The potential climatic problems engendered by anthropogenic CO_2 emissions have been widely debated and it is now accepted that fossil fuels must be replaced by greener sources of energy (1–3). This has prompted widespread research into solar energy, wind and wave power, geothermal energy, fuel cell technology, and renewable energy sources (3–7). Biomass is of particular interest as a sustainable energy source as it is neutral with respect to CO_2 emissions integrated over the annual growing cycle. Thus attempts have been made to harness gasified biomass (biogas), produced from partial oxidation/pyrolysis of bio-solids, for combined heat and power generation (CHP) (5–20). The fuel component of this "biogas" comprises about 9.8–17.2% CO, 9.8–13.2% H_2, and additional light hydrocarbons, e.g., CH_4 (5).

However, a major problem with biogas is that it also contains significant quantities of NH_3 (600–4000 ppm) produced from biogenic nitrogen (5). This NH_3 is a particular challenge since its combustion in a conventional burner results in the formation of significant amounts of environmentally harmful nitrogen oxides (NO_x) (21–24). Methods to overcome this problem have ranged from selective catalytic oxidation (8, 9, 11–18) and NH_3 decomposition (19, 20) to tail gas treatment (25–27) and water scrubbing (28). Selective catalytic combustion appears to be an attractive means of overcoming this problem as it does not require expensive secondary reactors (as in tail gas treatment) or produce large volumes of waste by-product (as in water scrubbing). Unfortunately to date the selectivity for the oxidation of NH_3 to N_2 is unsatisfactory, typically <70%, and significantly below the desired target level (8, 9, 11, 12, 18).

Conversely, as indicated, NH_3 is widely used industrially to reduce NO_x emissions by the Selective Catalytic Reduction process (SCR) (21, 25–27) following

$$NH_3 + NO + 1/4\,O_2 \rightarrow N_2 + 3/2\,H_2O. \qquad [1]$$

Indeed it has been previously demonstrated that the selective oxidation of NH_3 to N_2 over heteropoly acids and various Al_2O_3-supported oxides occurs via a similar mechanism, namely the *internal* (or *in situ*) SCR (*i*SCR) (13–16, 29–33). In this process a significant proportion of the NH_3 is oxidised to NO_x. However, this is then subsequently reduced by the remaining NH_3 to give N_2 in a highly selective reaction with yields in excess of 90%, significantly higher than has been reported in previous studies (8, 9, 11, 12, 18). This observation is consistent with the findings of Il'chenko and Golodets (29, 30) who suggested that N_2 formation occurs via the condensation of an imide (NH) and a nitroxyl

[1] To whom correspondence should be addressed. E-mail: b.w.l.southward@qub.ac.uk.

0021-9517/00 $35.00

(NHO). Moreover, the use of heteropoly acids (HPAs) in biogas clean up has illustrated that a catalyst, which coupled a strong Brønsted acid site with a redox centre, can facilitate adsorption and specific reaction of NH_3 to N_2 (13). This concept has been further extended to acidic zeolites, which also showed high N_2 yields, suggesting that the *i*SCR reaction may be a generic mechanism for the production of N_2 from NH_3 (16).

We have also recently demonstrated that N_2 may be formed in quantitative yield during biogas oxidation by taking advantage of a different mechanism, namely the coupled NH_3 oxidation/CO/H_2–NO_x reduction process (17). An important feature of this approach was the combination of process control, namely O_2 limitation, with a highly selective catalyst which preferentially oxidises NH_3 to NO_x even in the presence of a large excess of CO and H_2.

Unfortunately a limitation exists for reactions based upon either of these novel strategies because temperatures above 600°C are required. Thus a remaining challenge is to obtain high N_2 yields at much lower temperatures. In order to achieve this we have again combined the *i*SCR with process control to facilitate conversion of NH_3 to N_2 in biogas oxidation at low temperatures. This has been achieved by developing novel trapping catalysts which are operated in a cyclic mode with periodic switching between lean and rich (oxidising and reducing) conditions (34), in a similar manner to that employed in conventional NO_x trapping emission control catalysts (21, 35–38). This paper describes this new class of materials and compares the efficiency of N_2 production via the *i*SCR and NO reduction reactions under cyclic operating conditions.

2. EXPERIMENTAL

The catalysts were prepared by sequential incipient wetness impregnation of Al_2O_3 (CK300, Criterion Catalysts, BET 190 $m^2\,g^{-1}$, dried at 120°C for 14 h) with the required concentration of precursor: $BaNO_3$ 99%, $CuSO_4 \cdot 5H_2O$ 98% ex Aldrich and $PtDNDA_{aq}$ ex Johnson Matthey (2.28% Pt). After each impregnation the sample was dried in ambient air for 14 h, and then at 120°C for 24 h prior to calcination at 700°C for 6 h in static air.

All reactions were performed using 60 mg of sample in a conventional atmospheric pressure microreactor unit described previously (14). The reaction mixture was regulated by independent mass flow controllers giving the required gas compositions at a total flow of 300 $cm^3\,min^{-1}$ (equivalent to a gas hourly space velocity (GHSV) of ca. 240,000 h^{-1}). All gases were supplied by BOC (60 : 40 CO : H_2, 1% O_2/He, 20% O_2/He and 7000 ppm NO/He), except the 1% NH_3 in He, which was supplied by Air Products. All gases were used without further purification. Product analysis was by mass spectrometry (Hiden DSMS with appropriate corrections for m/z overlaps) with NO_x emissions and residual NH_3 levels being confirmed using an external oxidation reactor, with independent O_2 supply, coupled to a NO_x chemiluminescence detector (Signal series 4000 with data logging at 1 s intervals using Signal SIGLOG). Switching between lean and rich conditions was achieved using a pressure balanced 3-way valve to switch the oxidant from 20% O_2/He to 1% O_2/He. In all cases N_2 yield from NO_x readings is defined as $100 * ((NH_3\ \text{in}–NH_3\text{out})/NH_3\text{in})$, in the absence of any other N-containing product as determined by MS.

The interaction of adsorbates was examined by dosing 60 mg of sample with the required gas(es) in He for 15 min. The reactor was then purged for a further 15 min, prior to introduction of the second reaction mixture, as detailed in the text. The products formed were analysed by both MS and NO_x analysis and the total flow at all stages was 300 $cm^3\,min^{-1}$. All temperature programmed desorptions and reactions were performed using 60 mg of catalyst at a ramp rate of 10°C min^{-1} and total flow of 300 $cm^3\,min^{-1}$. Product analysis was again by a combination of MS and chemiluminescence.

3. RESULTS

(1) Initial Microreactor Trials

Figure 1 illustrates the N_2 production profiles for the 1%Pt–20%CuO–Al_2O_3 (PtCu), 1%Pt–20%BaO–Al_2O_3 (PtBa), and 1%Pt–Al_2O_3 (Pt) catalysts in the selective oxidation of NH_3 in a dilute fuel mixture (1.02% CO, 0.68% H_2) under lean steady state and cyclic operation (45 s lean/15 s rich). These data illustrate a clear beneficial effect of the promoter on N_2 selectivity even under steady state

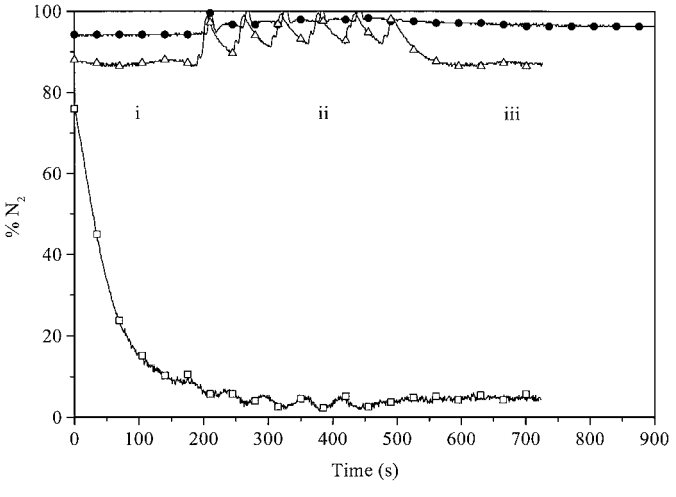

FIG. 1. Comparison of N_2 production from the selective catalytic oxidation of $NH_3/CO/H_2$ over (●) 1% Pt 20% CuO/Al_2O_3, (△) 1%Pt 20%BaO/Al_2O_3, and (□) 1%Pt/Al_2O_3 at 200°C (1000 ppm NH_3, 1.02% CO, 0.68% H_2, with either 2.05% O_2 (lean) or 0.1% O_2 (rich), balance He). Key: i, lean steady state operation; ii, cyclic operation 15 s rich/45 s lean; iii, final operation lean.

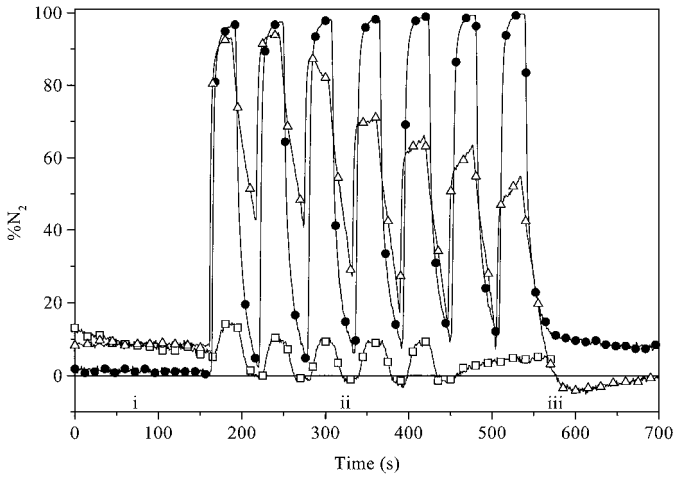

FIG. 2. Comparison of N_2 production from the selective catalytic oxidation of $NH_3/CO/H_2$ over (●) 1% Pt 20% CuO/Al_2O_3, (△) 1%Pt 20%BaO/Al_2O_3, and (□) 1%Pt/Al_2O_3 at 200°C (1000 ppm NH_3, 5.1% CO, 3.4% H_2, with either 9.3% O_2 (lean) 0.5% O_2 (rich), balance He). Key: i, lean steady state; ii, cyclic operation 30 s rich/30 s lean; iii, final operation lean.

conditions, with increases in N_2 production from ca. 5% for the Pt case to 94 and 87% for the PtCu and PtBa, respectively. For the latter two samples the N_2 selectivity was further enhanced by oxidant cycling giving peak N_2 yields of >99% in both cases. Note that for the PtCu catalyst, N_2 selectivity did not return immediately to the expected lean steady state value when switching was ceased but instead declined slowly over some 500 s to the original value. The Pt catalyst initially exhibited a high apparent NH_3 to N_2 conversion. However, this was found to be an experimental artefact and is only due to NH_3 adsorption: the true steady state N_2 yields were low (ca. 5%). In addition there was very little benefit observed when oxidant cycling was applied, again in marked contrast to both the PtCu and PtBa materials.

These experiments were performed with relatively low concentrations of the main fuel components (CO and H_2). We have previously shown that increasing the fuel concentration in the reaction mixture can result in a dramatic suppression of N_2 selectivity (39). This was again apparent in the activities of the promoted catalysts in a fuel mix containing higher concentrations of CO and H_2 (5.1% CO, 3.4% H_2, Fig. 2). Indeed for the PtCu sample the lean steady state N_2 yield declined from >90% (see Fig. 1) to essentially zero. However, as reported elsewhere (34), N_2 production could be restored by using cyclic conditions to give a peak yield of >97% N_2. Taking into account the minimum recorded during the lean phase, this material produced an average N_2 yield of ca. 60%, which, moreover, was stable throughout the whole period of the experiment. This behaviour is in marked contrast to that observed with both the Pt and PtBa materials. With the former there was a small increase (ca. 5% vs 8%) in steady state N_2 production compared to the reaction using the dilute feed, and this may possibly be due to NO–CO or NO–H_2 reactions. Once again the benefit of oxidant cycling was quite small for the Pt material, with N_2 production increasing from the steady state level to a maximum of some 15%, and even this small yield decreased with repeated cycling.

Similarly, while the activity of PtBa showed a marked enhancement initially during cycling (8% N_2 at steady state vs 94% by cycling), the yield of N_2 was found to decrease rapidly with cycle number. Hence after only 7 lean/rich cycles peak N_2 production was reduced to only 53%.

Upon returning the catalysts to steady state conditions it was noted that while both the Pt and PtBa samples exhibited NO_x desorption phenomena (resulting in an apparent negative N_2 production), the PtCu sample had a higher rate of N_2 production (ca. 8%) compared to the original value, i.e., comparable to the activity of the Pt or PtBa samples.

Additional information on the effect of cyclic operation was obtained from the analysis of all the reactants and products by MS. For the PtCu sample Fig. 3 shows the effect of changing from lean steady state to O_2 starvation conditions. Thus, under steady state lean conditions there was full combustion of the CO and H_2 with an associated exotherm of >45°C (as measured by an in-furnace thermocouple). Similarly, 100% NH_3 conversion was also observed but only at the expensive of N_2 selectivity since NO was produced almost exclusively, in agreement with the NO_x chemiluminescence results (see Fig. 2). However, upon switching to rich conditions, combustion essentially ceased and the breakthrough of CO and H_2 was apparent. Conversely, while NO production was similarly curtailed (Trace △), NH_3 breakthrough was not observed (Trace ◆). Unfortunately, due to the overlap of the MS signals for CO_2/N_2O (mz 44) and

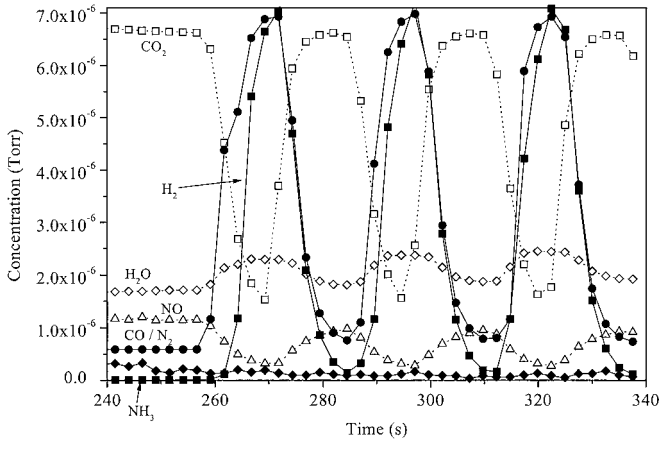

FIG. 3. Full MS conversion profiles from the selective catalytic oxidation of $NH_3/CO/H_2$ over 1% Pt 20% CuO/Al_2O_3 under cyclic operation at 200°C (1000 ppm NH_3, 5.1% CO, 3.4% H_2, with either 9.3% O_2 (lean) 0.5% O_2 (rich), balance He). Key: □, mz 44; △, mz 30 ∗ 10; ◇, mz 18; ●, mz 28; ◆, mz 17 ∗ 10; ■, mz 2.

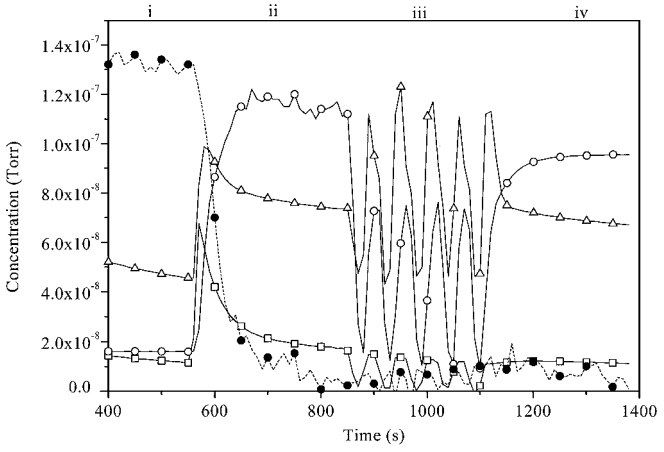

FIG. 4. Full MS product profiles from the selective catalytic oxidation of NH_3/H_2 over 1% Pt 20% CuO/Al_2O_3 at 200°C (1000 ppm NH_3, 6.0% H_2, with either 9.3% O_2 (lean) 0.5% O_2 (rich), balance He). Key: i, bypass; ii, initial reaction under lean conditions; iii, cyclic operation 30 s rich/30 s lean; iv, final reaction lean; ●, mz 17; □, mz 44; ○, mz 30; △, mz 28.

CO/N_2 (mz 28), neither the formation of N_2O as a by-product nor a corresponding increase in N_2 production could be determined. These results confirm the dramatic effect on N_2 selectivity of cyclic operation.

In order to be able to detect enhanced N_2 production, the PtCu catalyst was examined in a fuel stream containing only H_2–NH_3–O_2 (see Figs. 4 and 5). This confirmed both the high degree of conversion/trapping of NH_3 and the peaks in N_2 production during cyclic operation (Traces ● and △, respectively). Moreover, the reactivity of the sample under steady state was found to be markedly different in the absence of CO. The exotherm was only 18°C and, in addition, N_2 production was not suppressed to the same extent as in the NH_3–CO–H_2–O_2 reaction (23% vs 0% N_2), indicating that CO-derived species were involved in the inhibition of N_2 formation. The initial activity of the catalyst was also different with peaks at mz 28 and mz 44. Moreover, the signal at mz 44 decreased to background levels and indeed exhibited negative "peaks" during rich cycling, due to oxidation of CO-derived species in the MS analysis chamber, which contributes to the MS background at mz 44 only in the presence of O_2. Hence these observations confirm that under cyclic conditions there is minimal formation of N_2O. A further point of interest is the time delay between N_2 and NO peak values, with the latter occurring some 15 s later.

(2) Hybrid Bed Trials

As noted previously while the peak N_2 yields of the PtCu catalyst were very high, the integrated activity was somewhat lower, due to NO "slip" in the lean phase of the cycle. To address this issue we examined the activity of a hybrid bed system which coupled the PtCu and PtBa materials, with the role of the latter being to facilitate the reduction of trapped NO_x by CO and H_2 during the rich phase. The composite bed consisted of 45 mg of PtCu and 15 mg of PtBa as a secondary bed, separated by quartz wool. The performance of this hybrid system is illustrated in Fig. 6 (Trace ◆). The results demonstrate the improved performance during the lean part of the cycle (compare PtCu in Fig. 2). Hence there are improvements in both the lean steady state activity cf. PtCu (13% N_2 vs 0%) and in the minima during cyclic operation (ca. 35% N_2 vs ca. 9%). These improvements were also reflected in the integrated N_2 yield which increased from 60 to ca. 75% N_2. Attempts to further reduce

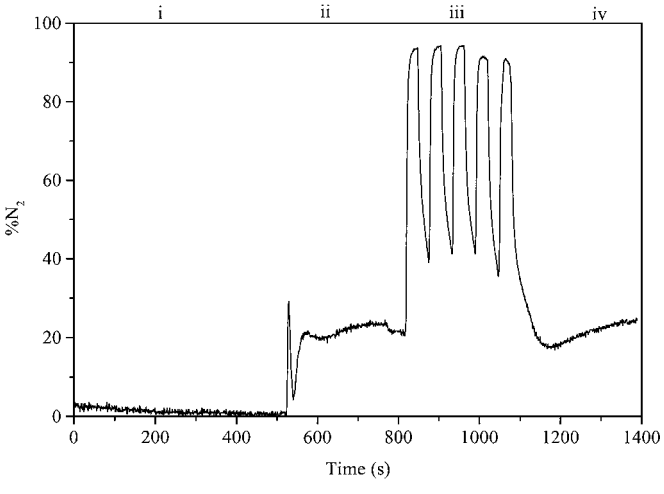

FIG. 5. N_2 production profile from the selective catalytic oxidation of NH_3/H_2 over 1% Pt 20% CuO/Al_2O_3 at 200°C (1000 ppm NH_2, 6.0% H_2, with either 9.3% O_2 (lean) 0.5% O_2 (rich), balance He). Key: i, bypass; ii, initial reaction under lean conditions; iii, cyclic operation 30 s rich/30 s lean; iv, final reaction lean.

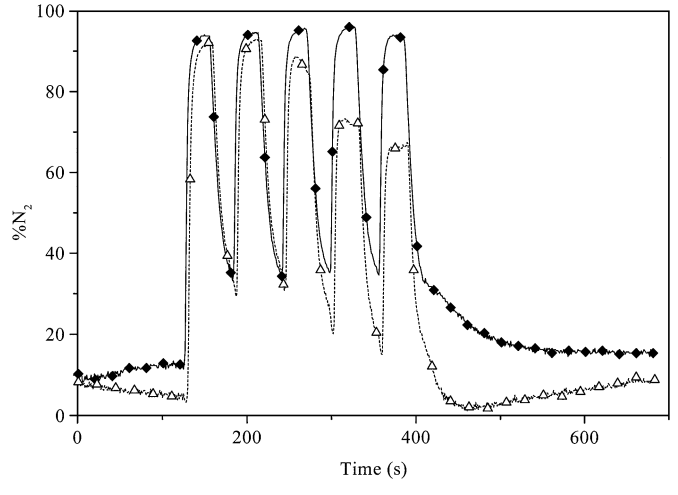

FIG. 6. Comparison of N_2 yields from the selective catalytic oxidation of $NH_3/CO/H_2$ over hybrid 1% Pt 20% CuO/Al_2O_3/1% Pt 20% BaO/Al_2O_3 catalysts at 200°C (1000 ppm NH_3, 5.1% CO, 3.4% H_2, with either 9.3% O_2 (lean) 0.5% O_2 (rich), balance He). Key: ◆, 45 mg PtCu: 15 mg PtBa; △, 30 mg PtCu: 30 mg PtBa.

TABLE 1

NH_3 TPD Results

	PtCu	PtBa	Pt
NH_3 Desorption max (°C)	243	274	274
Integrated NH_3 (Torr)	2.94×10^{-7}	1.56×10^{-7}	1.70×10^{-7}
N_2 desorption max (°C)	350	290, >625	290, 520
N_2O desorption max (°C)	—	290, >625	290, 560
NO desorption max (°C)	615	—	—

NO "slip" by using 30 mg of both PtCu and PtBa (Fig. 6, Trace △) were unsuccessful, with the activity becoming similar to that of pure PtBa. The integrated N_2 yield was only 51%.

(3) NH_3 TPD and Uptake Profiles

Based upon the kinetic measurements made using the PtCu sample, in particular the MS analysis, it appears that this material has a specific NH_3 trapping capability, which results in its ability to perform selective oxidation. To examine this possibility further, the NH_3 adsorption/desorption characteristics of the PtCu were examined by TPD and contrasted with those of the Pt and PtBa samples to determine whether this trapping function was a generic phenomenon or whether the PtCu has a specific activity (Fig. 7, Table 1). This analysis revealed similar uptake and desorption properties for the Pt and PtBa catalysts consistent with adsorption on Al_2O_3-based Brønsted acid sites (40). In contrast, PtCu exhibited a higher NH_3 uptake/desorption and, in addition, the temperature of the desorption maximum, ca. 243°C, was 30°C lower than for the Pt and PtBa.

The differences between the two classes of material were further reflected in their water and N-bearing product profiles, which are indicators of the extent of activation/oxidation of adsorbed NH_3. Both the Pt and PtBa exhibited large mz 18 peaks with a maximum at ca. 310°C, while the PtCu sample produced less mz 18 and had a desorption maximum of 390°C. Moreover, an examination of the N-containing products, arising from reduction of the oxidised surface during the initial dosing, also reflected differences in the sample. Hence while PtCu exhibited very small N_2 production peaks (not shown in Fig. 7 for sake of clarity) and a high-temperature NO peak, the PtBa and Pt samples evolved multiple N_2 and N_2O peaks. These data are consistent with the existence of a contribution to the adsorption of NH_3 (adsorption and retention of NH_x type species) on the copper component of PtCu.

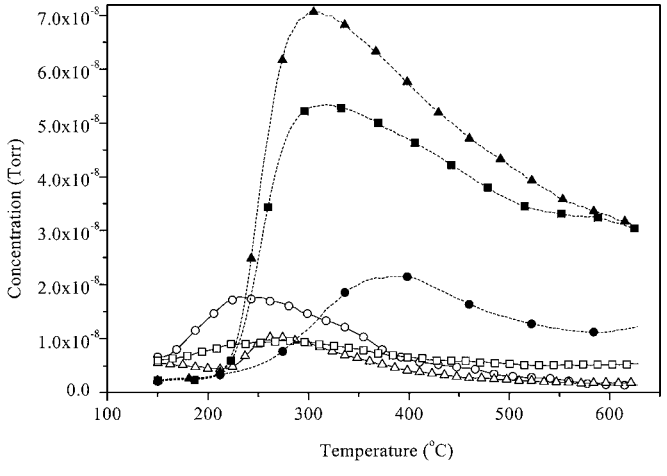

FIG. 7. NH_3/H_2O production TPD profiles. Key: ○, mz 17 Pt 20% CuO/Al_2O_3; □, mz 17 1%Pt/20% BaO/Al_2O_3; △, mz 17 1%Pt/Al_2O_3; ●, mz 18 PtCu; ▲, mz 18 PtBa; ■, mz 18 Pt.

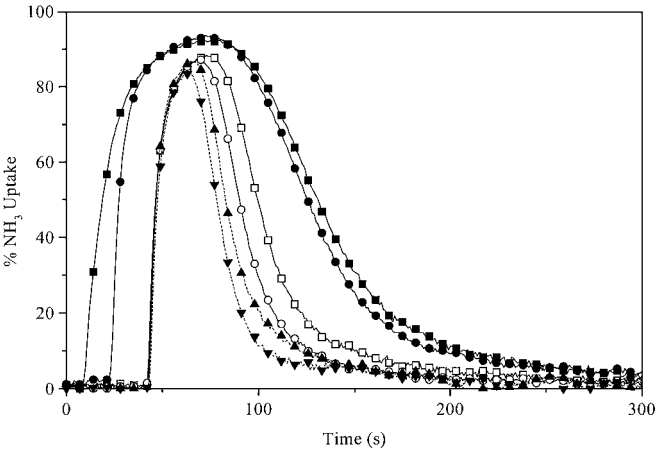

FIG. 8. NH_3 uptake profiles for PtCu. Key: ■, 1000 ppm NH_3 only at 100°C; ●, 1000 ppm NH_3, 5.1% CO, 3.4% H_2 at 100°C; □, 1000 ppm NH_3 only at 250°C; ○, 1000 ppm NH_3, 5.1% CO, 3.4% H_2 at 250°C; ▲, 1000 ppm NH_3 only at 300°C; ▼, 1000 ppm NH_3, 5.1% CO, 3.4% H_2 at 300°C.

However, NH_3 adsorption is dependent upon other variables, particularly under reaction conditions where CO and H_2 can competitively adsorb and where the exotherm of fuel combustion can significantly increase catalyst temperature. Therefore the temperature dependence of the NH_3 adsorption/desorption equilibrium was examined in the presence of CO/H_2 giving the results shown in Fig. 8 and summarised in Table 2.

Comparison of the NH_3 uptake profiles clearly shows negative effects on NH_3 adsorption. Indeed comparison of the best and worst cases (100°C with NH_3 alone, compared

TABLE 2

Effect of Temperature and CO/H_2 (8.5%) on NH_3 Uptake over PtCu

Temperature (°C)	NH_3 only (a.u.)	$NH_3/CO/H_2$ mix (a.u.)
100	11064	9744
250	5146	4364
300	3824	3186

Note. Based upon NO_x chemiluminescence data.

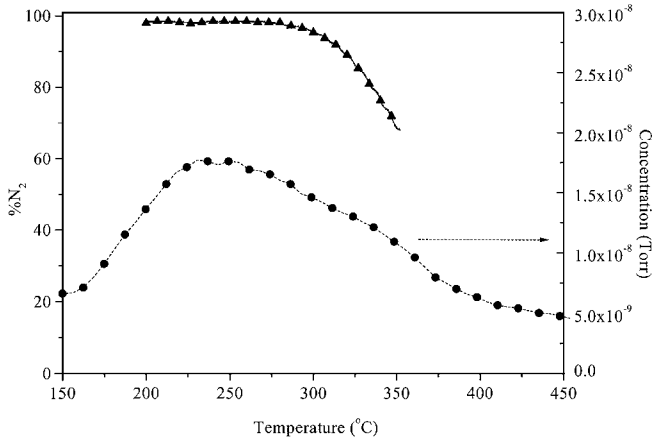

FIG. 9. Temperature profile for NH_3 oxidation and desorption over PtCu. Oxidation using 1000 ppm NH_3, 6.0% O_2. Key: ▲, N_2 production from NH_3 oxidation; ●, NH_3 TPD.

with 300°C with NH_3 in 5.1% CO and 3.4% H_2) shows that NH_3 uptake was reduced by approximately 70%. Similarly, the uptake at 300°C, both in the presence and absence of $CO + H_2$, was ca. 75% of the corresponding value at 250°C, while the presence of $CO + H_2$ reduced the adsorption at any given temperature by some 15%.

The kinetics of NH_3 oxidation are also important, since as the rate of NO_x formation increases, the possibility of NH_3 adsorption is reduced. Therefore, we have examined the temperature profile for NH_3 oxidation over PtCu (Fig. 9). In contrast to previous studies (8, 9, 11, 12, 14–16, 18), the sharp "volcano"-type profile in N_2 selectivity, typical of standard mono-site metal oxide *i*SCR catalysts, was not evident. Instead there is a plateau corresponding to a N_2 yield of >97% from 200°C to ca. 280°C. However, above these temperatures NO production increases significantly with 32% NO being observed at 350°C.

(4) Adsorbate Interactions

Although there is good agreement between the NH_3 uptake and TPD results regarding NH_x adsorption, NH_3 retention can only account for a limited amount of NH_3 removal, even under cyclic conditions. Thus this trapping must be coupled with a secondary process to facilitate the removal of the NH_x (the N_2 observed by MS in Fig. 4). To examine the possible reactions during cyclic operation the interactions between adsorbates and incoming gases on both PtCu and PtBa were examined to try and mimic real conditions. For example, under lean conditions the PtBa produces NO_x (Fig. 2), some of which is retained as $BaNO_3$ (18, 35–38). Hence exposure of this surface to rich conditions should, in theory, produce N_2. This "switch" was modelled by predosing the sample with NO/O_2, purging, and then introducing a reductant (NH_3 or CO/H_2 or H_2) while monitoring the evolution of any products by MS. The integrated production values for mz 28, 30, and 44 obtained from these experiments are summarised in Table 3.

TABLE 3

Summary of Adsorbate/Gaseous Species Interaction Results

Treatment	PtCu mass: concentration	PtBa mass: concentration
CO/H_2, purge, NO/He	mz 28: 7.34×10^{-09}	mz 28: 6.44×10^{-08} mz 44: 2.85×10^{-08}
NH_3, purge, NO/O_2	mz 28: 3.84×10^{-07} mz 44: 1.68×10^{-07}	mz 28: 1.88×10^{-07} mz 44: 9.50×10^{-08}
NO/O_2, purge, NH_3	mz 28: 2.25×10^{-08} mz 30: 5.89×10^{-09} mz 44: 4.47×10^{-09}	mz 28: 1.37×10^{-07} mz 44: 2.07×10^{-09}
NO/O_2, purge, H_2	mz 44: 3.12×10^{-09}	mz 28: 4.31×10^{-08} mz 30: 7.36×10^{-10}

These results reflect very different reactivities for the two catalysts. In the case of PtBa, mz 28 production peaks were found to occur in all reactions between adsorbate and secondary species. Subsequent re-examination by NO_x analysis confirmed the loss of NH_3 or NO, consistent with N_2 formation in all cases (Fig. 10 shows an example for NO introduction to PtBa pre-dosed with CO/H_2). Coincident with N_2 formation, significant levels of mz 44 production were noted for the NO ex CO/H_2, NO/O_2 ex NH_3, and NH_3 ex NO/O_2 cases. However, in general this could be ascribed the formation of CO_2. In addition, in the H_2 ex NO/O_2 case both N_2 and NO evolution were noted.

Conversely for the PtCu sample mz 28 production was an order of magnitude lower in all cases except for NO/O_2 dosing on an NH_3-treated surface where N_2 production was ca. twice that seen in the comparable PtBa case.

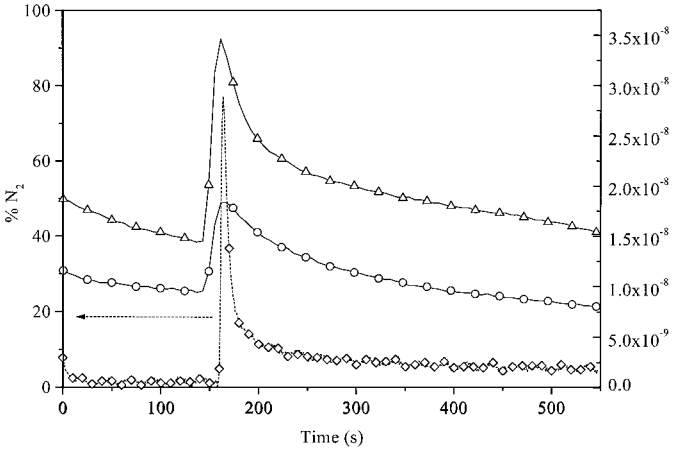

FIG. 10. N_2 production from NO exposure to PtBa catalyst ex CO/H_2 at 200°C. Key: ◇, % N_2 from chemiluminescence; △, mz 28 from MS; ○, mz 44 from MS.

4. DISCUSSION

From the results obtained the following points may be drawn:

(i) N_2 may be formed selectively under steady state lean burn conditions with Pt catalysts modified by addition of BaO or CuO although the selectivity is strongly suppressed in the presence of high concentrations of fuel components, particularly CO. This contrasts markedly with the unmodified Pt–Al_2O_3 catalyst which exhibited low N_2 selectivity under all conditions.

(ii) Cyclic operation restores N_2 selectivity, even in the presence of a large excess of CO and H_2, over both PtCu and PtBa, although the latter shows a marked deterioration in activity with time. In contrast, extended operation under lean or rich conditions results in NO_x formation and trap saturation, respectively (34).

(iii) At low temperatures PtCu appears to be able to trap NH_x species, with minimal activation/oxidation of the NH_3: the extent of NH_x trapping is dependent on the catalyst temperature and the partial pressure of CO and H_2. Conversely, PtBa is able to selectively adsorb and retain NO_x.

(iv) Multiple N_2-producing reactions can occur on PtBa between adsorbates and gaseous species, and these are typical of the species expected to be present during cyclic operation. For PtCu these interactions are far less pronounced except in the case of the reaction of NO/O_2 on an NH_3-treated surface where significant production of N_2 is observed.

(v) The use of a hybrid PtCu/PtBa dual bed system enhances integrated N_2 yield by reducing NO "slip" during the lean cycle of operation without compromising activity during rich operation.

These results reflect a complex interplay between the Pt and the oxide modifier and demonstrate that manipulation on the molecular level can dramatically alter the activity of a catalyst. Moreover they show that process control can again be utilised to "force" the catalyst to adapt and perform the required selective reactions much more effectively (17, 41). To facilitate discussion of the results we propose the model (for PtCu) illustrated in Fig. 11.

First, we consider the high N_2 yields observed under lean steady state operation. Both the PtCu and PtBa gave >85% N_2 in the presence of low concentrations of CO and H_2. This is both significantly higher than previously reported (8, 9, 11, 12, 18) and, more importantly, a massive increase compared to the unmodified Pt catalyst which only gave N_2 yields ranging from 29% N_2 at 200°C in the absence of fuel to 8% N_2 when low concentrations of CO and H_2 were present. The activity is also markedly different from that of 10% Cu–Al_2O_3 which required $T \geq 400$°C to facilitate selective N_2 production (34).

These improvements in N_2 yields are ascribed to the establishment of an Internal Selective Catalytic Reduction (*i*SCR) mechanism (13–16, 29–33). The *i*SCR arises because the PtCu and PtBa catalysts act as composite materials that facilitate reaction by a synergy between different types of active site.

Clearly the precise modes of action differ for the PtCu and PtBa but the underlying principle is similar and involves the combination of an oxidised N-bearing species (e.g., NO_x) with a reduced N-bearing species (e.g., NH_x). In the case of PtCu we suggest that this reaction occurs between NH_x species adsorbed on the CuO (consistent with the data presented herein and with previous *in situ* DRIFTS studies (31)) and NO_x formed from NH_3 oxidation on the Pt, as observed in both dilute fuel (Fig. 1) and NH_3 oxidation temperature profile experiments (Fig. 9). *In terms of the proposed model, this mode of action corresponds to state e in Fig. 11.* The presence of the oxidised N species is particularly important, as NH_3 activation has been demonstrated to be rate limiting in the selective oxidation of NH_3 (14, 29–31), consistent with the lower activity but high selectivity of CuO–Al_2O_3 (29, 30, 34). Similarly the need for the reduced N-bearing species is reflected by the decreasing N_2 selectivity in standard NH_3 oxidation above 300°C, i.e., temperatures above the NH_3 TPD maximum (Fig. 9). This premise correlates well with the activity of zeolitic materials for NH_3 oxidation and NO reduction where again N_2 and NO formation/slip were dependent on the concentration of adsorbed NH_3 (16, 41).

In contrast, for the PtBa catalyst, Pt again oxidises NH_3 to NO_x, but this is then adsorbed on the BaO and subsequently reduced to N_2 (21, 35–38). Based upon the adsorbate interaction results (Table 3, Fig. 10), it is clear that the reductant can be NH_3 or CO or H_2, or indeed a combination of all three. However, the extent of N_2 production was found to decrease in the order $NH_3 > CO > H_2$, which suggests that NH_3 may be the primary reductant. This is unsurprising given the need for recombination of N-containing species if CO or H_2 reduce the $NO_{x(ads)}$, and the kinetic results which show near quantitative NH_3 conversion to N_2 for steady state lean oxidation of dilute fuel. However, given the significantly higher concentrations of CO and H_2 it is difficult to ascribe the reduction exclusively to an *i*SCR-type reaction.

When the concentration of CO and H_2 is increased these inter-related processes are unbalanced and low N_2 yields are recorded under lean state steady conditions, corresponding to state a in Fig. 11. This arises because of the altered nature of the process under examination. In this case the combustion of the high concentrations of CO and H_2 dramatically raises the temperature of the catalyst bed to >300°C, which completely alters the balances of the processes responsible for N_2 selectivity. This issue is an entirely new factor in the consideration of selective NH_3 oxidation in biogas as all

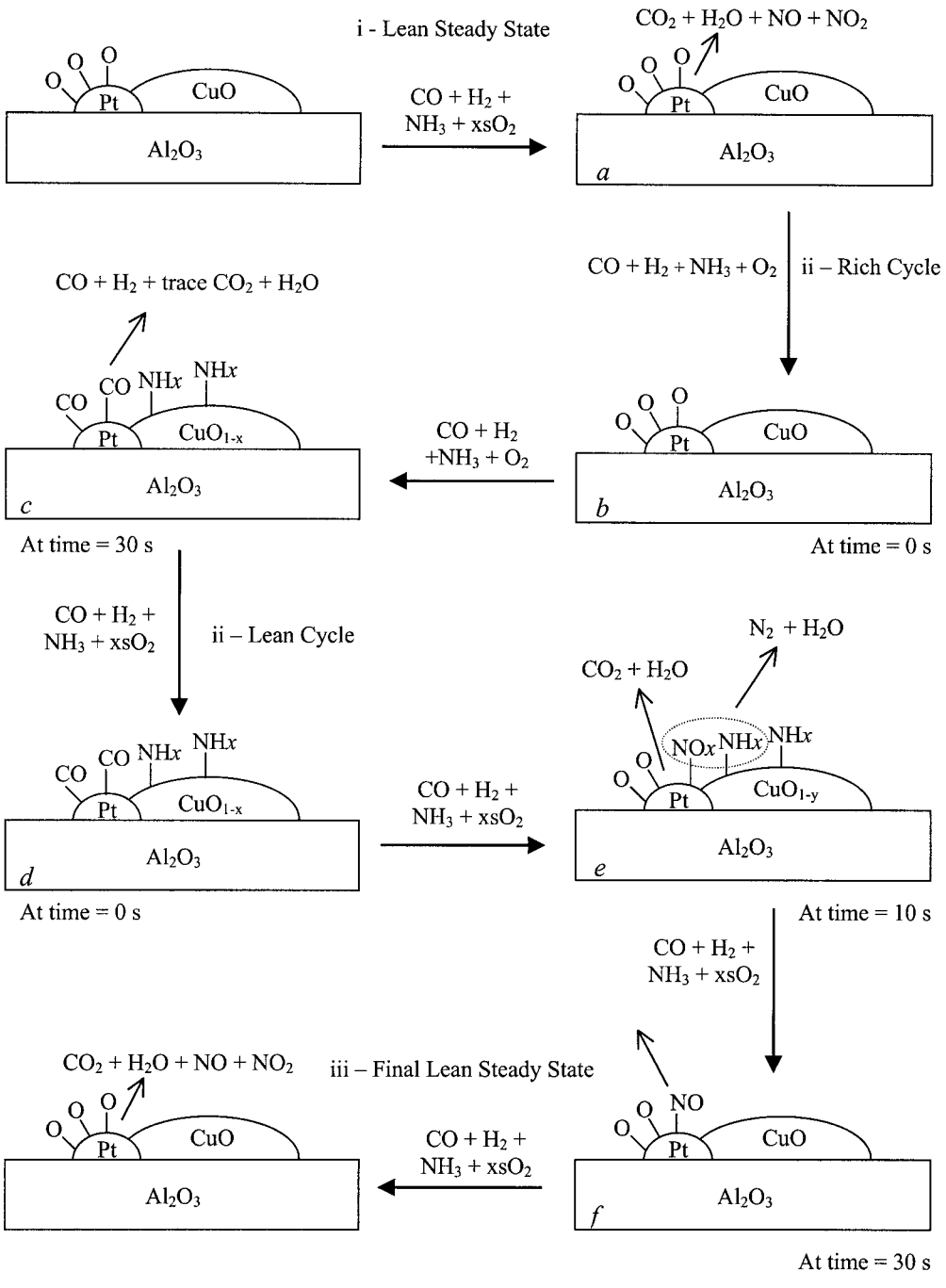

FIG. 11. Proposed model of N_2 production during cyclic operation on the PtCu catalyst.

previous studies have either examined dilute fuel streams at low gas hourly space velocities (8, 9, 11, 12, 15, 16, 18) or O_2 free/limited reactions (17, 19, 20), which in all cases ameliorate the exotherm. Moreover, since the activation of NH_3, which is critical for N_2 production, is coincident with light-off it is not possible to avoid this issue by catalyst modification.

Thus in the lean steady state reaction with high levels of CO and H_2 the combustion exotherm facilitates desorption of NH_3 from the CuO as seen in TPD and also reduces NH_3 uptake (Figs. 7 and Fig. 8, Table 2, respectively), thereby removing the reductant required to reduce the NO formed on the Pt. As indicated previously this is consistent with the loss in N_2 selectivity observed for NH_3 oxidation in the absence of fuel (Fig. 9 and previous work (14–16)). In addition, the rate of NH_3 oxidation to NO_x on Pt is also increased, decreasing the concentration of NH_3 available to replenish the CuO trapping component. Moreover as the temperature

increases, the ability of CuO to oxidise NH_3 also becomes significant, and the trap itself becomes an active site (29, 30, 34). Finally the situation is further exacerbated by the presence of large local partial pressures of CO and H_2 which also inhibit NH_3 adsorption (Fig. 8, Table 2).

Similarly for the H_2–O_2–NH_3 reaction, steady state N_2 production was lower than found with low concentrations of $CO + H_2$ but higher than found with high concentrations of $CO + H_2$ (Figs. 4 and 5), while the measured external exotherm was approximately half of that observed for the CO/H_2 case.

These exothermic factors can also affect the activity of the PtBa which under high fuel lean conditions displays an identical reactivity to Pt. Here again the in-bed exotherm resulting from fuel combustion destroys the balance required for N_2 selectivity. Again the exotherm reduces nitrogen reagent uptake, in this case NO_x, and again promotes desorption from the trapping oxide as indicated by Fridell *et al.* (37) and Mahzoul and co-workers (38). N_2 selectivity is further decreased by the significantly enhanced oxidation rate for all components at the higher catalyst temperature thus removing any available reductants before any interaction with the BaO can occur.

However, the introduction of oxidant cycling reestablishes N_2 selectivity and *i*SCR-type mechanisms for both catalysts, corresponding to states b–e in Fig. 11 for PtCu. Thus as the catalyst is exposed to rich conditions there is a marked decrease in catalyst temperature due to the cessation of combustion and the associated exotherm. This reestablishes the equilibrium in favour of NH_3 adsorption (with an associated partial reduction) of the CuO, again as a nonactivated NH_x type moiety, consistent with TPD and MS reaction profiles (Table 1, Figs. 3 and 8). This trapping avoids NH_3 "slip" during the rich phase and regenerates the active adsorbed reduced-N necessary for the *i*SCR. Upon returning the catalyst to lean conditions full combustion is reestablished and the active oxidised-N species produced on the Pt effectively "titrate" adsorbed NH_x on the CuO_{1-x} yielding N_2 coincident with reoxidation of the trap ($CuO_{1-x} \rightarrow CuO_{1-y} \rightarrow CuO$). Obviously this process is dependent upon coverage of the trap by NH_x and, as these species are depleted, given that replenishment by $NH_{3(g)}$ becomes increasing unfavourable as the catalyst temperature increases due to the combustion exotherm, NO breakthrough occurs (state f). This is consistent with adsorbate studies which reflect the high reactivity of an NO/O_2 mixture on an NH_x covered surface (Table 2). It may also explain the low initial lean steady state N_2 selectivity, as the CuO phase of the fresh catalyst contained no trapped NH_x species.

Conversely, in the case of the PtBa the mode of action is similar to that of a conventional NO_x trapping system (21, 35–38). Thus, during lean operation the Pt again provides an active site for the oxidation of NH_3 to NO_x. The NO_x is stored on the BaO and reduced during the rich phase. Moreover, upon returning the catalyst to lean conditions significant amounts of the "new" NO_x formed are trapped, which accounts for the higher apparent activity during the lean cycle as compared with PtCu. However, with time this process is less effective than the process on PtCu, as reflected in the decreasing peak N_2 yields observed. This decrease is ascribed to a combination of factors. First, during the lean cycle comparatively high levels of NO_x are produced, ca. 900 ppm, cf. standard trapping studies (37, 38). Second cyclic operation results in both a lower average O_2 concentration, due to switching, and lower catalyst temperature as compared with steady state lean conditions, due to transient exotherm effects, both of which mitigate against NO_x trapping (35–38). Finally during initial operation NO_x adsorption can also occur on Al_2O_3 as has been demonstrated by Burch *et al.* (42, 43). However, this mechanism provides a limited and nonregenerable contribution to NO_x removal, and upon saturation of the support a further contribution to NO_x output occurs. Hence as switching is initiated, there is a higher internal catalyst temperature, due to the exotherm, a high initial O_2 partial pressure, and free Al_2O_3–based adsorption sites. All of these positive characteristics enhance initial activity, but as support saturation occurs and cycling decreases both the exothermic contribution from combustion and the average O_2 concentration, total NO_x uptake decreases, which in turn results in a decrease in N_2 production during rich regeneration.

The benefits of cyclic operation are emphasised in the activity of the hybrid bed system. The hybrid catalyst also reflects the benefits of the different modes of operation of the two trapping materials and integrates their strengths to obtain maximum integrated N_2 yields. Thus peak N_2 yields during the rich cyclic exceed 95%, due to the trapping/*i*SCR mechanism occurring on PtCu described previously, while the PtBa reduces NO_x "slip" during the rich phase. Moreover, these enhancements were obtained at effective GHSVs of 320,000 h^{-1} and 960,000 h^{-1} for the PtCu and PtBa sections of the hybrid bed, reflecting the extremely rapid nature of the processes involved.

5. CONCLUSIONS

The selective low-temperature oxidation of NH_3 to N_2 in simulated biogas is possible using Pt-based trapping catalysts in conjunction with cyclic oxidant operation. Two possible paths for N_2 production are possible. The first occurs on 1%Pt–20%CuO–Al_2O_3 and involves an *i*SCR type reaction between NO_x formed on the Pt which is reduced to N_2 by NH_x adsorbed on the CuO. A second mechanism, which occurs on 1%Pt–20%BaO–Al_2O_3, involves the reduction of NO_x trapped on the BaO by a combination of NH_3, CO, and H_2. The efficiency of these reactions can be markedly influenced by catalyst temperature, which is dramatically

increased during combustion of high concentrations of fuel components during lean cycle operation. Cyclic operation minimises the adverse effects of this exotherm and reestablishes the delicate balance of trapping and reaction to restore high N_2 yields. Coupling of these two trapping materials and mechanisms in a hybrid system results in optimum low-temperature performance, with peak cycle N_2 yields >95% and integrated N_2 production of ca. 75% over the rich/lean cycle.

ACKNOWLEDGMENTS

We are pleased to acknowledge the financial support of ABB-Alstom, the DTI, and EPSRC through the FORESIGHT Challenge initiative. Helpful discussions with Dr. M. Amblard (Lens), Cranfield University (Mr. J. J. Witton, Professor B. Moss, Mr. J. M. Przybylski, and Dr. E. Noordally) and at ABB-Alstom (Mr. M. Cannon and Mr. G. Kelsall) are gratefully acknowledged.

REFERENCES

1. "Kyoto Protocol to the United Nations Framework Convention on Climate Change," Kyoto, Japan, 1–10 December 1997.
2. R. T. Watson, M. C. Zinyowera, R. H. Moss (Eds.), "The Regional Impacts of Climate Change, An Assessment of Vulnerability," special report of the International Panel on Climate Change working group, Cambridge Univ. Press, Cambridge, UK, 1997.
3. United States Environmental Protection Agency/White House Initiative on Global Climate Change factsheet. http://www.whitehouse.gov/Initiatives/Climate/main.html and related sites.
4. Titus, J. G., Kuo, C. Y., Gibbs, M. J., LaRoche, T. B., Webb, M. K., and Waddell, J. O., *J. Water Res. Planning Management* **113**(2), 1987.
5. "Development of Improved Stable Catalysts and Trace Element Capture for Hot Gas Cleaning," DTI/ETSU/Clean Coal Power Generation Group, Project Profile 178, 1996.
6. Energie Helpline UK newsletter on the EU 5th Framework Programme for cleaner, renewable and more economic energy, c/o Telegraphic House, Waterfront Quay, Salford Quays, Manchester, M25 2XW.
7. DTI New Review quarterly newsletter for the UK New and Renewable Energy Industry, issue 42, November 1999, ETSU, Harwell, Didcot, Oxon, OX11 0RA UK.
8. Lietti, L., Groppi, G., and Ramella, C., *Catal. Lett.* **53**, 91 (1998).
9. Zwinkels, M. F. M.,Eloise Heginuz, G. M., Gregertsen, B. H., Sjöström, K., and Järås, S. G., *Appl. Catal. A* **148**, 325 (1997).
10. Pfefferle, W. C., Belgian Patent, 814752, 1974.
11. Johansson, E. M., and Järås, S. G., *Catal. Today* **47**, 359 (1999).
12. Lietti, L., Ramella, C., Groppi, G., and Forzatti, P., *Appl. Catal. B* **21**, 89 (1999).
13. Burch, R., and Southward, B. W. L., *Chem Commun.* 1475 (1999).
14. Amblard, M., Burch, R., and Southward, B. W. L., *Appl. Catal. B* **22**, L159 (1999).
15. Amblard, M., Burch, R., and Southward, B. W. L., *Catal. Today* **59**, 365 (2000).
16. Amblard, M., Burch, R., and Southward, B. W. L., *Catal. Lett.* **68**, 105 (2000).
17. Burch, R., and Southward, B. W. L., British Patent Application 98238879.3, 1998; Burch, R., and Southward, B. W. L., *Chem. Commun.* 702 (2000).
18. Johansson, E. M., Berg, M., Kjellström, K., and Järås, S. G., *Appl. Catal. B* **20**, 319 (1999).
19. Mojtahedi, W., and Abbasian, J., *Fuel* **74**, 1698 (1995).
20. Simell, P., Kurkela, E., Ståhlberg, P., Hepola, J., *Catal. Today* **27**, 55 (1996).
21. Fritz, A., and Pitchon, V., *Appl. Catal. B* **13**, 1 (1997).
22. "Urban Air Quality in the United Kingdom," First Report of the Quality of Air Quality Group, Dept. of the Environment, 1993.
23. Zeldovich, J., *Acto Physiochem. USSR* **21**, 577 (1946).
24. "Ozone in the United Kingdom 1993," Third Report of the UK Photochemical Oxidants Review Group, Dept. of the Environment, 1993.
25. Vatcha, S. R., *Eng. Conv. Waste Managmt.* **38**, 1327 (1997).
26. Heck, R., *Catal. Today* **53**, 519 (1999).
27. Busca, G., Lietti, L., Ramis, G., and Berti, F., *Appl. Catal. B* **18**, 1 (1998).
28. Kaspar, J., Clausen, C. A., and Cooper, C. D., *J. Air Waste Managmt. Assoc.* **46**, 127 (1996).
29. Il'chenko, N. I., and Golodets, G. I., *J. Catal.* **39**, 57 (1975).
30. Il'chenko, N. I., and Golodets, G. I., *J. Catal.* **39**, 73 (1975).
31. Amblard, M., Ph.D. thesis, University of Reading (1999).
32. Janssen, F. J. J. G., van den Kerkhof, F. M. G., Bosch, H., and Ross, J. R. H., *J. Phys. Chem.* **91**, 5921 (1987).
33. Janssen, F. J. J. G., van den Kerkhof, F. M. G., Bosch, H., and Ross, J. R. H., *J. Phys. Chem.* **91**, 6633 (1987).
34. Burch, R., and Southward, B. W. L., *Chem Commun.* 1115 (2000).
35. Toyota Patent EP 573 672A1 (1992).
36. Farrauto, R. J., and Heck, R. M., *Catal. Today* **51**, 351 (1999).
37. Fridell, E., Skoglundh, M., Westerberg, B., Johansson, S., and Smedler, G., *J. Catal.* **183**, 196 (1999).
38. Mahzoul, H., Brilhac, J. F., and Gilot, P., *Appl. Catal. B* **20**, 47 (1999).
39. Amblard, M., Burch, R., and Southward, B. W. L., "Clean Catalytic Combustion of N-Bearing Gasified Biomass," Fourth International Workshop on Catalytic Combustion, San Diego, 1999.
40. Rodriguez, L. M., Alcaraz, J., Hernandez, M., Dufaux, M., Ben Taarit, Y., and Vrinat, M., *Appl. Catal. A* **189**, 53 (1999).
41. Richter, M., Eckelt, R., Parlitz, B., and Fricke, R., *Appl. Catal. B* **15**, 129 (1998).
42. Burch, R., Halpin, E., and Sullivan, J. A., *Appl. Catal. B* **17**, 115 (1998).
43. Burch, R., Fornasiero, P., and Southward, B. W. L., *J. Catal.* **182**, 234 (1999).